Novel Schemes for Hyperbolic PDEs Using Osmosis Filters from Visual Computing

Kai Hagenburg, Michael Breuß, Joachim Weickert, and Oliver Vogel

Mathematical Image Analysis Group,
Faculty of Mathematics and Computer Science,
Building E1.1, Saarland University, 66041 Saarbrücken, Germany,
{hagenburg,breuss,weickert,vogel}@mia.uni-saarland.de
http://www.mia.uni-saarland.de

Abstract. Recently a new class of generalised diffusion filters called osmosis filters has been proposed. Osmosis models are useful for a variety of tasks in visual computing. In this paper, we show that these filters are also beneficial outside image processing and computer graphics: We exploit their use for the construction of better numerical schemes for hyperbolic partial differential equations that model physical transport phenomena.
Our novel osmosis-based algorithm is constructed as a two-step, predictor-corrector method. The predictor scheme is given by a Markov chain model of osmosis that captures the hyperbolic transport in its advection term. By design, it also incorporates a discrete diffusion process. The corresponding terms can easily be identified within the osmosis model. In the corrector step, we subtract a stabilised version of this discrete diffusion. We show that the resulting osmosis-based method gives correct, highly accurate resolutions of shock wave fronts in both linear and nonlinear test cases. Our work is an example for the usefulness of visual computing ideas in numerical analysis.

Key words: diffusion filtering, osmosis, diffusion-advection, drift-diffusion, hyperbolic conservation laws, finite difference methods, predictor-corrector schemes, stabilised inverse diffusion

1 Introduction

Hyperbolic differential equations (HDEs) model physical wave propagation and transport processes. An important feature of solutions to such partial differential equations (PDEs) is the formation of discontinuities, also called shocks. In image processing shocks correspond to edges. Therefore, it seems natural that concepts from the numerical approximation of HDEs can be useful for constructing discrete filters that deal with the sharpening or evolution of edges. Rudin and Osher [1, 2] have exploited this idea to define edge-enhancing processes. They use the same mechanism as in HDEs to model so-called shock filters. When dealing with noisy images, one often aims at preserving or enhancing edges, while in homogeneous image regions a smoothing should take place. Corresponding to this idea, combinations of shock filters with mean curvature motion [3] or with nonlinear diffusion [4] have been developed. Also, the concept of stabilised

inverse diffusion (SID) has inspired interesting developments, both in a linear [5, 6] and a nonlinear setting [7–9]. In particular, concepts from the numerics of HDEs such as suitable combinations of one-sided differences have been applied to stabilise discretisations of inverse diffusion [5, 9]. Similar ideas from the numerics of HDEs dealing with an improved shock resolution have also been used for optical flow computations [10].

While the influence of ideas from the numerics of HDEs on the field of image processing is undeniable, up to now there are not many works that use techniques from image analysis for improving numerical methods for HDEs. In [11–13] higher order discretisations of HDEs that give a sharp shock resolution but suffer from oscillations are combined with anisotropic diffusion filtering. There, anisotropic diffusion is used to smooth oscillations without destroying the shocks. As an alternative procedure, one may employ a classic first-order scheme featuring diffusive errors to capture the hyperbolic transport. Then, in a second step, the artificial blurring can be removed by linear or nonlinear SID. This methodology is actually older than the SID-approach in image processing, and it is called flux-corrected transport (FCT) [14]. Modern variations of it have been developed for applications in image processing [15–17] and the numerics of HDEs [18].

Our Contribution. The discussion above shows that so far only diffusion or inverse diffusion processes have been used to correct numerical errors in schemes for HDEs. The goal of the present paper is to propose a novel construction of predictor-corrector schemes for HDEs that introduces a different mechanism. To this end, we make use of the recently introduced class of osmosis filters for visual computing problems [19]. They can be regarded as nonsymmetric generalisation of diffusion filters that involve a hyperbolic advection term which allows numerous applications beyond classic diffusion filtering. In contrast to all previous works, we do not correct the numerical errors of a classic HDE scheme by a diffusion filter, but we employ the hyperbolic term of the osmosis process for predicting the hyperbolic transport in the HDE. The Markov chain model corresponding to osmosis filters also includes a diffusion component. In the context of HDEs, this is a reasonable feature, since it is well-known that numerical schemes must incorporate a diffusive mechanism to approximate nonlinear shocks at the correct position, cf. [20]. However, since this diffusion also blurs shocks, we supplement in a corrector step SID to counter this undesired diffusion. As a benefit of the osmosis model, we can do this in a straight forward fashion on a completely discrete basis; see [16] for a similar use of this technique. In linear and nonlinear test cases, we compare our method to a classic second-order MUSCL-Hancock scheme [21, 22] which gives typical results for solvers in the field of HDEs. However, while the MUSCL-Hancock scheme has a similar predictor-corrector format as our proposed method, our approach is substantially easier to implement and much more efficient. We confirm that our osmosis-based algorithm is not only competitive in quality to the MUSCL-Hancock scheme, it even gives much sharper approximations at shocks.

Paper Organisation. In Section 2, we briefly review diffusion filtering and its generalisation to osmosis filters. Then we show in Section 3 how to use osmosis models to design novel predictor-corrector schemes for a fundamental class of HDEs, namely hyperbolic conservation laws. In Section 4, we present numerical experiments. The paper is finished with a conclusion in Section 5.

2 Diffusion Filters and Osmosis

Diffusion filters. Let a continuous-scale 1-D signal $u(x,t)$ be given where we associate x and t with space and time. The diffusion PDE with positive diffusivity function $g(x,t)$ reads in 1D as

$$\partial_t u \;=\; \partial_x \left(g \, \partial_x u \right). \tag{1}$$

It has to be supplemented with an initial condition $u(x,0) := f(x)$, and in case of a bounded domain also with boundary conditions.

In a discrete setting, we use a spatial mesh width h and define the pixel location x_i by $x_i := (i-1/2)h$ for $i \in \{1,\dots,N\}$. Analogously, we introduce a time discretisation $t_k = k\tau$, so that we obtain a discrete signal $u_i^k \approx u(x_i,t_k)$. Then a standard finite difference discretisation of (1) is given by the explicit scheme

$$\frac{u_i^{k+1}-u_i^k}{\tau} \;=\; \frac{1}{h}\left(g_{i+1/2}^k \frac{u_{i+1}^k - u_i^k}{h} \;-\; g_{i-1/2}^k \frac{u_i^k - u_{i-1}^k}{h} \right) \tag{2}$$

where $g_{i+1/2}^k$ denotes the diffusivity between the computational cells i and $i+1$.
Using the mesh ratio $r := \frac{\tau}{h^2}$, our scheme can be rewritten as

$$u_i^{k+1} \;=\; u_i^k - r g_{i+1/2}^k u_i^k - r g_{i-1/2}^k u_i^k + r g_{i+1/2}^k u_{i+1}^k + r g_{i-1/2}^k u_{i-1}^k. \tag{3}$$

It is convenient to express this as a matrix-vector multiplication of the form $\boldsymbol{u}^{k+1} = \boldsymbol{Q}^k \boldsymbol{u}^k$, where $\boldsymbol{Q}^k$ is an $(N \times N)$-matrix with entries

$$q_{i,j}^k := \begin{cases} 1 - r g_{i-1/2}^k - r g_{i+1/2}^k & (j=i) \\ r g_{i-1/2}^k & (j=i-1) \\ r g_{i+1/2}^k & (j=i+1) \\ 0 & \text{(else)}. \end{cases} \tag{4}$$

Let us briefly review some important properties of the matrix $\boldsymbol{Q}^k$; cf. [23]. Obviously, the matrix is symmetric. Stability of the iterative scheme (3) can be shown if the entries of $\boldsymbol{Q}^k$ are nonnegative. Since the diffusivity is positive, all off-diagonals contain nonnegative entries, leaving only the diagonal entries without proper clarification. Therefore, for all diagonal entries it must hold that

$$q_{i,i}^k \;=\; 1 - r g_{i-1/2}^k - r g_{i+1/2}^k \;\geq\; 0. \tag{5}$$

This implies a stability condition on the time step size τ.
In order to implement homogeneous Neumann boundary conditions $\partial_x u = 0$, we modify the entries for $q_{1,1}^k$ and $q_{N,N}^k$ such that

$$q_{1,1}^k \;:=\; 1 - r g_{3/2}^k \quad \text{and} \quad q_{N,N}^k \;:=\; 1 - r g_{N-1/2}^k. \tag{6}$$

This can be interpreted as setting the missing terms $g_{1/2}^k$ and $g_{N+1/2}^k$ to 0. It should be mentioned that it is also possible to implement Dirichlet boundary conditions or periodic boundary conditions.

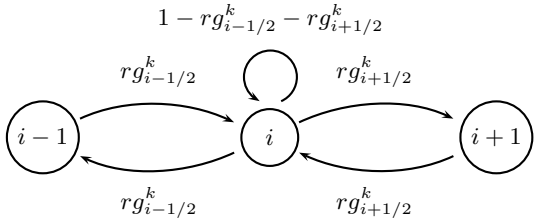

Fig. 1. Diffusion process visualised in terms of a Markov chain model.

Furthermore, it holds that the sums over all entries in each column of $\boldsymbol{Q}^k$ equal 1. By the symmetry of $\boldsymbol{Q}^k$ this also holds for the row sums. Both properties have an effect on the evolution of the process: The unit column sums imply the preservation of the average grey value. With the unit row sums it is possible to prove a discrete maximum-minimum principle. Moreover, in [23] it is shown that the evolution converges to a constant steady state that is identical to the average grey value of the initial signal. Let us stress that the properties of the discrete minimum-maximum-principle and the trivial steady state solution are consequences of the symmetry of $\boldsymbol{Q}^k$ which implies that unit column sums are equivalent to unit row sums.

We can also express diffusion using Markov chains. Markov chains are described in terms of stochastic matrices that incorporate transition probabilities [24]. A stochastic matrix is a matrix with only nonnegative entries and unit column sums. By taking into account the positivity of the diffusivity and choosing a mesh ratio r such that (5) is satisfied for all i, we can ensure that the matrix $\boldsymbol{Q}^k$ contains only nonnegative entries. Moreover, all column sums are 1. Thus, $\boldsymbol{Q}^k$ is a stochastic matrix, and the entries $q^k_{i,j} \geq 0$ can be interpreted as transition probabilities. In the Markov chain setting it is convenient to use a graph-based representation of the diffusion model. It is given in Figure 1.

Osmosis as a generalisation of diffusion filters. Following [19] let us now consider a nonsymmetric extension of diffusion that is called osmosis. To this end, we assume that we have semi-permeable membranes between adjacent pixels. An osmosis process permits selective transport of particles such that the transition probabilities may be different, depending on the orientation. For example, the transition probability from pixel i to pixel $i+1$ may differ from the transition probability from pixel $i+1$ to pixel i. In the Markov model, this leads to the loss of the symmetry in the graph in Figure 1. This is achieved by allowing different diffusivities in different orientation. Such oriented diffusivities are called *osmoticities*. The forward osmoticity from pixel i to $i+1$ at time level k is denoted by $g^{+,k}_{i+1/2}$, while $g^{-,k}_{i+1/2}$ is the backward osmoticity from pixel $i+1$ to i. We choose these osmoticities such that the normalisation condition

$$g^{+,k}_{i+1/2} \;+\; g^{-,k}_{i+1/2} \;=\; 2 \tag{7}$$

is fulfilled for all i; cf. [19]. Since osmoticities are also supposed to be nonnegative, we conclude that in this case their range is in $[0, 2]$.

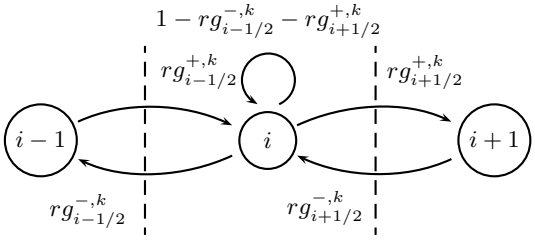

Fig. 2. Osmosis process visualised in terms of a Markov chain model.

In Figure 2 we see a graph-based representation of osmosis. This new process is expressed by the scheme

$$u_i^{k+1} \;=\; u_i^k \underbrace{- rg^{+,k}_{i+1/2} u_i^k \;-\; rg^{-,k}_{i-1/2} u_i^k}_{\text{“outflow”}} \underbrace{+ rg^{-,k}_{i+1/2} u_{i+1}^k \;+\; rg^{+,k}_{i-1/2} u_{i-1}^k}_{\text{“inflow”}} \tag{8}$$

This can be rewritten in matrix-vector notation $\boldsymbol{u}^{k+1} = \boldsymbol{P}^k \boldsymbol{u}^k$ with a matrix $\boldsymbol{P}^k := (p^k_{i,j})$ with

$$p^k_{i,j} \;:=\; \begin{cases} 1 - rg^{-,k}_{i-1/2} - rg^{+,k}_{i+1/2} & (j = i) \\ rg^{+,k}_{i-1/2} & (j = i-1) \\ rg^{-,k}_{i+1/2} & (j = i+1) \\ 0 & \text{(else).} \end{cases} \tag{9}$$

Homogeneous Neumann boundary conditions are implemented by setting the osmoticities in the boundary locations $x_{1/2}$ and $x_{N+1/2}$ to 0.

Let us comment on the structure of $\boldsymbol{P}^k$. As in the case with $\boldsymbol{Q}^k$, the system matrix (9) is a stochastic matrix if r is chosen such that the diagonal entries of $\boldsymbol{P}^k$ are nonnegative. Since $\boldsymbol{P}^k$ has unit column sums, it follows that osmosis preserves the average grey value:

$$\frac{1}{N}\sum_{i=1}^N u_i^{k+1} \;=\; \frac{1}{N}\sum_{i=1}^N \sum_{j=1}^N p^k_{i,j} u_j^k \;=\; \frac{1}{N}\sum_{j=1}^N \underbrace{\left(\sum_{i=1}^N p^k_{i,j}\right)}_{=1} u_j^k \;=\; \frac{1}{N}\sum_{j=1}^N u_j^k. \tag{10}$$

However, $\boldsymbol{P}^k$ is not symmetric. Thus, unit row sums cannot be guaranteed. As a consequence, a discrete maximum-minimum principle does not hold, but the nonnegativity of $\boldsymbol{P}^k$ still implies that a nonnegative initial signal remains nonnegative after filtering. More importantly, the lack of symmetry allows that osmosis can lead to nontrivial steady states. This interesting property is analysed in detail in [19], where it is also exploited for many applications.

As proven in [19], the scheme (8) with normalisation condition (7) approximates on a fixed, given mesh of size h the *1-D osmosis PDE*

$$\partial_t u \;+\; \partial_x \left(\frac{g^+ - g^-}{h} u \right) \;=\; \partial_{xx} u \tag{11}$$

Fig. 3. Seamless image cloning with osmosis (with permission from [19]). From left to right: **(a)** Original painting of Euler. **(b)** Original drawing of Lagrange (with to-be-cloned face selected). **(c)** Direct cloning on top of Euler's head. **(d)** Cloning with osmosis image editing. See [19] for more details.

where g^+ and g^- are continuous-scale representations of the osmoticities. PDEs of this type are called *advection-diffusion equations* or *drift-diffusion equations*.

It is straight forward to extend osmosis to higher dimensions and colour images; see [19] for details. In [19] it is also shown that osmosis constitutes a versatile framework for many visual computing problems such as clustering, data integration, focus fusion, exposure blending, image editing, shadow removal, and compact image representation. Fig. 3 illustrates this. Let us now explore a new application field for osmosis that goes beyond visual computing tasks: the construction of better numerical schemes for hyperbolic conservation laws.

3 Osmosis Schemes for HDEs

Hyperbolic conservation laws. We aim at constructing numerical approximations of HDEs that can be written as

$$\partial_t u \;+\; \partial_x(\phi(u)) \;=\; 0. \tag{12}$$

Such equations are called *hyperbolic conservation laws (HCLs)*. This is a fundamental class of PDEs with many applications in science and engineering [25]. The design of numerical schemes for HCLs can easily be transferred to other specific HDEs. The function ϕ in (12) is called *flux function*. Its properties, like e.g. linearity or convexity, are important for the features one can expect from solutions of such PDEs. We will write ϕ in the format of a velocity times the underlying density function, i.e. $\phi(u) = au$, where $a := a(u)$ may be nonlinear. This is a very basic choice in the field of HCLs, naturally arising in many settings [25].

Comparing the differential formula for osmosis (11) with the general form of HCLs (12), one can immediately identify the flux $\phi(u)$ and the corresponding flux within the osmosis advection term

$$\phi(u) \;=\; \frac{g^+ - g^-}{h}\, u. \tag{13}$$

In addition, there is the diffusion term $\partial_{xx} u$. The general idea we pursue in the following is to determine useful expressions for g^+ and g^-, so that we can capture the hyperbolic transport by the osmosis model.

Selection of the osmoticities. For the general construction of osmosis-based algorithms, we stick for simplicity to the 1-D situation. The methodology can be extended to the 2-D case in a straight forward fashion.

In order to approximate the flux $\phi(u) = a(u)u$ of the hyperbolic transport contained in (11), we choose as osmoticities

$$g^{+,k}_{i+1/2} \;:=\; 1 \;+\; \frac{h\, a^k_{i+1/2}}{2} \qquad \text{and} \qquad g^{-,k}_{i+1/2} \;:=\; 1 \;-\; \frac{h\, a^k_{i+1/2}}{2} \tag{14}$$

with velocities $a^k_{i+1/2}$ defined at pixel borders. This setting makes the osmotic transport identical to the desired format $a(u)u$. Let us discuss two examples.

– *Example 1: Osmoticities for linear advection.*
The linear advection equation

$$\partial_t u \;+\; \alpha\, \partial_x u \;=\; 0 \tag{15}$$

is a standard example of HDEs, defined via $\phi(u) := \alpha u$ with $\alpha \in \mathbb{R}$. In order to approximate (15), we set all velocities $a^k_{i+1/2}$ to the same value α.

– *Example 2: Osmoticities for Burgers' equation.*
Burgers' equation is a classic test case for nonlinear HDEs:

$$\partial_t u \;+\; \partial_x \left(\frac{1}{2}\, u^2 \right) \;=\; 0, \qquad \text{i.e. } \phi(u) \;=\; \frac{1}{2}\, u^2. \tag{16}$$

Rewriting the flux in the format $\phi(u) = a(u)\, u$ leads to the discrete expression

$$a^k_{i+1/2} \;=\; a(u^k_i, u^k_{i+1}) \;:=\; \frac{1}{2}\, \frac{u^k_i + u^k_{i+1}}{2} \tag{17}$$

after approximating the density $u^k_{i+1/2}$ at the border between pixels i and $i+1$ by averaging.

Subtracting the diffusion. Our osmosis scheme contains the diffusive term $\partial_{xx} u$ which leads to an additional smoothing of the signal. In order to compensate for this effect, we apply a method similar to the fully discrete SID step in [17].

If we use our definitions of $g^{\pm}_{i\pm1/2}$ from (14) within the osmosis filter (8) and carry out further computations, we obtain

$$\begin{aligned} \tilde{u}^k_i \;=\; & \underbrace{u^k_i \;-\; \frac{\tau}{h} \left(a^k_{i+1/2}\, \frac{u^k_{i+1} + u^k_i}{2} - a^k_{i-1/2}\, \frac{u^k_i + u^k_{i-1}}{2} \right)}_{(A)} \\ & +\; \underbrace{r\, (u^k_{i+1} - 2u^k_i + u^k_{i-1})}_{(B)}. \end{aligned} \tag{18}$$

The term (A) corresponds to the update formula of an explicit scheme for discretising the hyperbolic transport, while (B) is a discretisation of a time step performed with linear diffusion. It should be noted that (18) varies from the standard Lax-Friedrichs scheme by controlling the diffusive part (B) with the same time step size τ as the transport term (A), see also [25–27].

Let us now subtract the effect of the latter by performing a SID step in the same style as in [16, 17]. This gives the total, corrected result

$$u_i^{k+1} \;:=\; \tilde{u}_i^k - c_{i+1/2}^k + c_{i-1/2}^k \tag{19}$$

where $c_{i\pm1/2}^k$ denote the fluxes of the stabilised inverse diffusion:

$$c_{i+1/2}^k \;:=\; \mathrm{minmod}\left(\tilde{u}_i^k - \tilde{u}_{i-1}^k,\; \eta_{i+1/2}^k \left(\tilde{u}_{i+1}^k - \tilde{u}_i^k\right),\; \tilde{u}_{i+2}^k - \tilde{u}_{i+1}^k\right) \tag{20}$$

with the minmod function

$$\mathrm{minmod}(a,b,c) := \begin{cases} \max(a,b,c) & \text{if } a>0 \text{ and } b>0 \text{ and } c>0 \\ \min(a,b,c) & \text{if } a<0 \text{ and } b<0 \text{ and } c<0 \\ 0 & \text{else.} \end{cases} \tag{21}$$

Thereby, $\eta_{i+1/2}^k := r$ is the antidiffusion coefficient, as identified in (B). The other arguments of the minmod function serve as stabilisers.

The complete algorithm. Now we can summarise our method in a nutshell.

Osmosis-based Method for Approximating $\partial_t u + \partial_x(\phi(u)) = 0$.
Step 1: Determine the velocity function a for a given flux function $\phi(u) = a(u)u$.
Step 2: Compute the osmoticities according to (14).
Step 3: Perform one predictor step by applying the osmosis scheme (18).
Step 4: Perform the corrector step (19).
Step 5: Repeat steps 2 to 4 until the stopping time is reached.

4 Numerical Experiments

We illustrate the quality of our osmosis-based algorithm with several standard examples from the field of HDEs. Thereby, we focus our attention on the shocks that are the most interesting features of hyperbolic PDEs.

For comparison with standard methods for HDEs, we employ a second-order high-resolution MUSCL-Hancock method [21, 22]. This classic method gives typical results for high-resolution solvers in this field.

Linear advection in 1D. In our first experiment we consider the linear advection equation (15) with $\alpha = 1$ and periodic boundary conditions. We apply it for transporting a box-like initial signal

$$f(x) := \begin{cases} 1 & (10 \le x < 30) \\ 0 & (\text{else}). \end{cases} \tag{22}$$

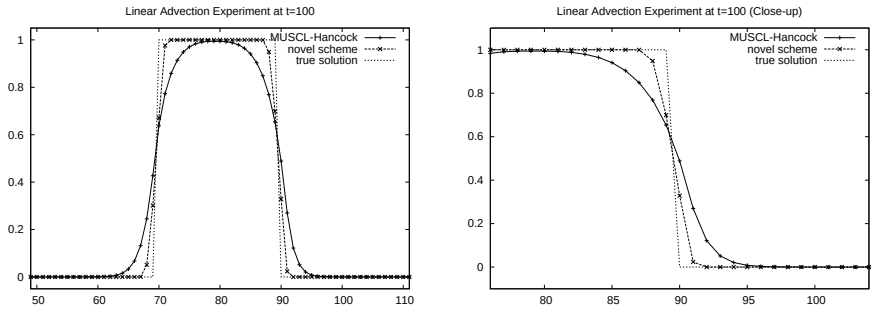

Fig. 4. Linear advection experiment. **(a) Left:** Results at $t = 60$. **(b) Right:** Close-up on the right edge of the signal.

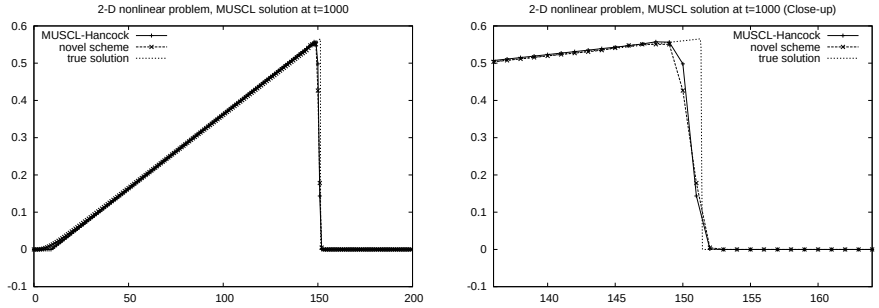

Fig. 5. Burgers' Equation. **(a) Left:** Results at $t = 250$. **(b) Right:** Close-up on the right edge of the signal.

As numerical parameters we choose $N := 200$, $h := 1$, and $\tau := 0.25$. In Figure 4 we show a snapshot taken after 240 time steps of numerical solutions computed by our new scheme and the reference method, together with the exact solution. We observe that our osmosis method gives much sharper discontinuities than the MUSCL-Hancock scheme and comes closer to the exact solution.

Nonlinear Burgers' equation in 1D. Now we consider the Burgers' equation (16) under the same parameter settings and the same initial condition as in the first test. By the nonlinear evolution, the box signal is shifted to the right. The discontinuity at the right hand side of the box travels as a shock while the rest of the signal is gradually shifted, transforming the box into a ramp. Figure 5 shows the numerical solutions at $t = 250$ for our osmosis-based scheme as well as for the MUSCL-Hancock implementation, together with the exact solution. Both methods give reasonable approximations in this test case.

Nonlinear 2D experiment. As already mentioned, extending osmosis to 2D is straight forward: One only has to define osmoticities as proposed in (14) for x- and y-direction. Note that our resulting scheme is rotationally invariant w.r.t. the diffusion part, since this is given in 2D by the isotropic Laplace operator [19]. The 2-D MUSCL-

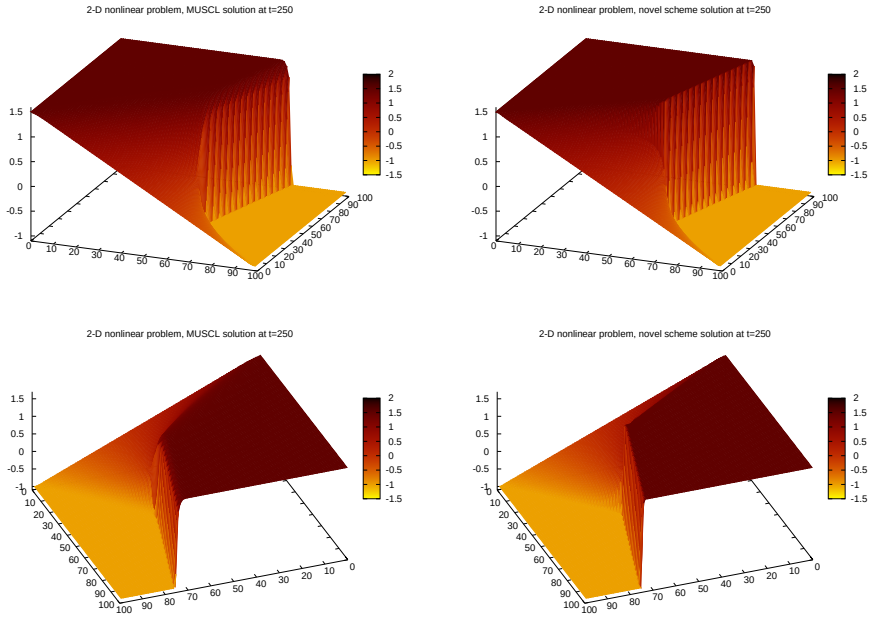

Fig. 6. Steady-state result for the 2-D test. **Left:** MUSCL-Hancock scheme. **Right:** Osmosis scheme. **Top row:** Top-down view. **Bottom row:** Different angle, showing the shock region in detail.

Hancock scheme is presumably comparable in this respect, as it uses information from a diamond-shaped stencil of 13 nodes [21, 22].

For our 2-D experiment we consider the nonlinear problem from [11] where the steady state is sought. It combines Burgers' equation with linear advection by choosing the flux function $\phi(u) = \frac{1}{2}u^2$ in x-direction, and $\psi(u) = u$ in y-direction. As initial state on our domain $[0, 100] \times [0, 100]$ we take

$$f(x,y) := \begin{cases} 1.5 & (x = 1) \\ -2.5x + 1.5 & (y = 1) \\ -1 & (x = 100) \\ 0 & (\text{else}). \end{cases} \tag{23}$$

These values also define non-zero Dirichlet boundary conditions on three borders of our domain. On the remaining border (at $y = 100$) we impose homogeneous Neumann boundary conditions. We implement the process in a straight forward way using the osmoticities for Burgers' equation and linear advection in x- and y-direction, respectively. The problem is discretised on a grid of size 100×100, and the numerical steady state obtained at $t = 250$ is depicted in Fig. 6. In the smooth regions, our method performs comparable to the MUSCL-Hancock scheme, but we obtain a much sharper shock resolution.

5 Conclusion

We have developed a novel class of schemes for approximating HCLs. They combine recently developed osmosis filters for resolving transport with a stabilised inverse diffusion step. We have shown the strength of our approach for resolving solutions with shocks, which are important features in the fields of hyperbolic differential equations.

Quite frequently, new results in visual computing benefit from the use of modern techniques from numerical analysis. Our work is an example for a fertilisation in the inverse direction. Note that the key for obtaining the results in our paper is the use of a very recent technique from visual computing. However, we do not only propose a novel construction of numerical schemes for HDEs, we also introduce a new application of osmosis filters. Therefore, this paper is an example for the useful interaction of visual computing ideas and numerical analysis. In our future work we will investigate if also other modern PDE-based methods from image analysis can be used with benefit in numerical analysis.

Acknowledgments. The authors gratefully acknowledge the funding given by the *Deutsche Forschungsgemeinschaft* (DFG), grant We2602/8-1.

References

1. Rudin, L.I.: Images, Numerical Analysis of Singularities and Shock Filters. PhD thesis, California Institute of Technology, Pasadena, CA (1987)
2. Osher, S., Rudin, L.I.: Feature-oriented image enhancement using shock filters. SIAM Journal on Numerical Analysis **27** (1990) 919–940
3. Alvarez, L., Mazorra, L.: Signal and image restoration using shock filters and anisotropic diffusion. SIAM Journal on Numerical Analysis **31** (1994) 590–605
4. Kornprobst, P., Deriche, R., Aubert, G.: Image coupling, restoration and enhancement via PDEs. In: Proc. 1997 IEEE International Conference on Image Processing. Volume 4., Washington, DC (October 1997) 458–461
5. Osher, S., Rudin, L.: Shocks and other nonlinear filtering applied to image processing. In Tescher, A.G., ed.: Applications of Digital Image Processing XIV. Volume 1567 of Proceedings of SPIE. SPIE Press, Bellingham (1991) 414–431
6. Breuß, M., Welk, M.: Analysis of staircasing in semidiscrete stabilised inverse linear diffusion algorithms. Journal of Computational and Applied Mathematics **206** (2007) 520–533
7. Pollak, I., Willsky, A.S., Krim, H.: Image segmentation and edge enhancement with stabilized inverse diffusion equations. IEEE Transactions on Image Processing **9**(2) (February 2000) 256–266
8. Gilboa, G., Sochen, N.A., Zeevi, Y.Y.: Forward-and-backward diffusion processes for adaptive image enhancement and denoising. IEEE Transactions on Image Processing **11**(7) (2002) 689–703
9. Welk, M., Gilboa, G., Weickert, J.: Theoretical foundations for discrete forward-and-backward diffusion filtering. In Tai, X.C., Mørken, K., Lysaker, M., Lie, K.A., eds.: Scale-Space and Variational Methods in Computer Vision. Volume 5567 of Lecture Notes in Computer Science. Springer, Berlin (2009) 527–538
10. Breuß, M., Zimmer, H., Weickert, J.: Can variational models for correspondence problems benefit from upwind discretisations? Journal of Mathematical Imaging and Vision **39**(5) (2011) 230–244

11. Grahs, T., Meister, A., Sonar, T.: Image processing for numerical approximations of conservation laws: nonlinear anisotropic artificial dissipation. SIAM Journal on Scientific Computing **23**(5) (2002) 1439–1455
12. Grahs, T., Sonar, T.: Entropy-controlled artificial anisotropic diffusion for the numerical solution of conservation laws based on algorithms from image processing. Journal of Visual Communication and Image Representation **13**(1/2) (2002) 176–194
13. Wei, G.: Shock capturing by anisotropic diffusion oscillation reduction. Computer Physics Communications **144** (2002) 317–342
14. Boris, J.P., Book, D.L.: Flux corrected transport. I. SHASTA, a fluid transport algorithm that works. Journal of Computational Physics **11**(1) (1973) 38–69
15. Burgeth, B., Pizarro, L., Breuß, M., Weickert, J.: Adaptive continuous-scale morphology for matrix fields. International Journal of Computer Vision **92**(2) (2011) 146–161
16. Breuß, M., Weickert, J.: A shock-capturing algorithm for the differential equations of dilation and erosion. Journal of Mathematical Imaging and Vision **25** (2006) 187–201
17. Breuß, M., Weickert, J.: Highly accurate schemes for PDE-based morphology with general structuring elements. International Journal of Computer Vision **92**(2) (2011) 132–145
18. Breuß, M., Brox, T., Sonar, T., Weickert, J.: Stabilized nonlinear inverse diffusion for approximating hyperbolic PDEs. In Kimmel, R., Sochen, N., Weickert, J., eds.: Scale-Space and PDE Methods in Computer Vision. Volume 3459 of Lecture Notes in Computer Science., Berlin, Springer (2005) 536–547
19. Weickert, J., Hagenburg, K., Vogel, O., Breuß, M., Ochs, P.: Osmosis models for visual computing. Technical report, Department of Mathematics, Saarland University, Saarbrücken, Germany (2011)
20. LeVeque, R.J.: Numerical Methods for Conservation Laws. Birkhäuser, Basel (1992)
21. van Leer, B.: Towards the ultimate conservative difference scheme, V. A second order sequel to Godunov's method. Journal of Computational Physics **32**(1) (1979) 101–136
22. Toro, E.F.: Riemann Solvers and Numerical Methods for Fluid Dynamics - A Practical Introduction. 2nd edn. Springer, Berlin (1999)
23. Weickert, J.: Anisotropic Diffusion in Image Processing. Teubner, Stuttgart (1998)
24. Seneta, E.: Non-negative Matrices and Markov Chains. Springer Series in Statistics. Springer, Berlin (1980)
25. LeVeque, R.J.: Finite Volume Methods for Hyperbolic Problems. Cambridge University Press, Cambridge, UK (2002)
26. Breuß, M.: The correct use of the Lax-Friedrichs method. ESAIM: Mathematical Modeling and Numerical Analysis **38**(3) (2004) 519–540
27. Breuß, M.: An analysis of the influence of data extrema on some first and second order central approximations of hyperbolic conservation laws. ESAIM: Mathematical Modeling and Numerical Analysis **39**(5) (2005) 965–993